

Mechanism suppressing glycogen synthesis in neurons and its demise in progressive myoclonus epilepsy

David Vilchez¹, Susana Ros¹, Daniel Cifuentes¹, Lluís Pujadas¹, Jordi Vallès¹, Belén García-Fojeda², Olga Criado-García², Elena Fernández-Sánchez², Iria Medraño-Fernández², Jorge Domínguez¹, Mar García-Rocha¹, Eduardo Soriano¹, Santiago Rodríguez de Córdoba^{2,3} & Joan J Guinovart^{1,3}

Glycogen synthesis is normally absent in neurons. However, inclusion bodies resembling abnormal glycogen accumulate in several neurological diseases, particularly in progressive myoclonus epilepsy or Lafora disease. We show here that mouse neurons have the enzymatic machinery for synthesizing glycogen, but that it is suppressed by retention of muscle glycogen synthase (MGS) in the phosphorylated, inactive state. This suppression was further ensured by a complex of laforin and malin, which are the two proteins whose mutations cause Lafora disease. The laforin-malin complex caused proteasome-dependent degradation both of the adaptor protein targeting to glycogen, PTG, which brings protein phosphatase 1 to MGS for activation, and of MGS itself. Enforced expression of PTG led to glycogen deposition in neurons and caused apoptosis. Therefore, the malin-laforin complex ensures a blockade of neuronal glycogen synthesis even under intense glycogenic conditions. Here we explain the formation of polyglucosan inclusions in Lafora disease by demonstrating a crucial role for laforin and malin in glycogen synthesis.

Glucose is the main source of energy in the brain; however, glycogen is not stored in neurons and is present only in astroglial cells¹. Nevertheless, in several pathologies, polymers of glucose, normally referred to as polyglucosan bodies, accumulate in neuronal tissue². One such pathology is Lafora-type progressive myoclonus epilepsy^{3–5} (EPM2, OMIM 254780). The hallmark of Lafora disease is the presence of large inclusions (Lafora bodies) in the axons and dendrites of neurons^{6,7}. These inclusions are composed of poorly branched polymers of glucose, which can be considered to be abnormal glycogen molecules. However, the mechanism by which polyglucosan bodies accumulate in Lafora disease remains unknown. Lafora disease typically manifests during adolescence with generalized tonic-clonic seizures, myoclonus, absences, drop attacks or partial visual seizures. As the disease progresses, afflicted individuals suffer a rapidly progressive dementia with apraxia, aphasia and visual loss, leading to a vegetative state and death, usually in the first decade from the onset of the initial symptoms. Seizures are commonly the first manifestation of the disease and may be generalized (tonic-clonic, absences, myoclonic, tonic or atonic) or focal (usually with visual symptoms). Electroencephalograms show both generalized and focal epileptiform discharges^{8–13}.

Lafora disease is inherited as an autosomal recessive disorder and shows genetic heterogeneity. It has been associated with mutations in two genes. *Epilepsy, progressive myoclonus 2a* (*EPM2A*) is mutated in approximately 48% of individuals with Lafora disease and encodes laforin, a dual-specificity protein phosphatase with a functional carbohydrate-binding domain^{14–18}. A second gene, *Epilepsy, progressive*

myoclonus 2b (*EPM2B*), is mutated in 30–40% of those with Lafora disease and encodes malin, an E3 ubiquitin ligase^{18–20}. Malin interacts with laforin and causes its ubiquitination²⁰. Individuals with mutations in laforin or malin are neurologically and histologically indistinguishable, which strongly suggests that these two proteins operate through common physiological pathways¹⁸.

To examine how defects in either laforin or malin contribute to the formation of Lafora bodies, we have examined their role in neurons. We show that the laforin-malin complex blocks glycogen synthesis in these cells by inducing the proteasome-dependent degradation of MGS and PTG.

RESULTS

Neurons keep the machinery for glycogen synthesis inactive

Analysis of whole mouse brain, differentiated mouse Neuro2a (N2a) cells and primary cultured mouse neurons showed that neurons express MGS (**Fig. 1a,b**). Expression of the liver glycogen synthase (LGS) isoform was absent in these specimens (**Fig. 1a** and data not shown). Furthermore, neurons did not express glycogen phosphorylase, the enzyme that is responsible for the degradation of this polysaccharide (**Fig. 1b**). Notably, despite the expression of MGS, neurons and N2a cells did not accumulate detectable amounts of glycogen when cultured in medium containing high concentrations of glucose (30 mM) (**Fig. 1c**). In contrast, astrocytes grown under the same conditions showed marked accumulation of this polysaccharide (**Fig. 1c**; see ref. 1).

¹Institute for Research in Biomedicine and University of Barcelona, Barcelona Science Park, Josep Samitier 1-5, E-08028 Barcelona, Spain. ²Centro de Investigaciones Biológicas, Consejo Superior de Investigaciones Científicas, Ramiro de Maeztu 9, E-28040 Madrid, Spain. ³These authors contributed equally to this work. Correspondence should be addressed to J.J.G. (guinovart@pcb.ub.es) and S.R.d.C. (SRdeCordoba@cib.csic.es).

Received 9 August; accepted 21 September; published online 21 October 2007; doi:10.1038/nn1998

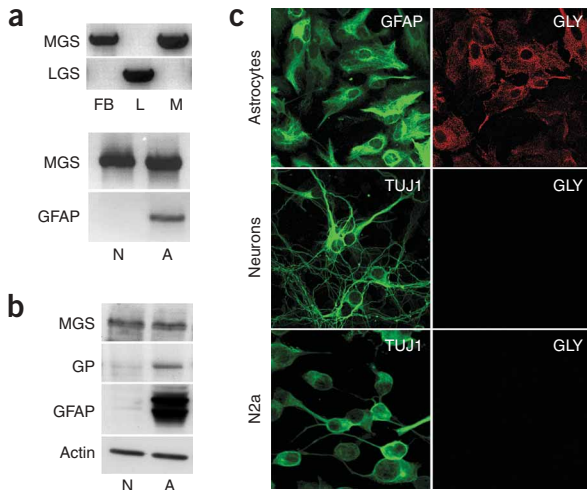


Figure 1 Neurons express MGS, but do not accumulate glycogen. (a) Upper, RT-PCR analysis of MGS and LGS in mouse forebrain (FB), liver (L) and muscle (M). Lower, RT-PCR analysis of MGS in primary cultures of neurons (N) and astrocytes (A). GFAP was used as an astroglial marker. Note the absence of signal in neurons. (b) Western blot analysis of homogenates of primary cultured neurons and astrocytes with antibodies to MGS, glycogen phosphorylase (GP) and GFAP. The astrocyte marker GFAP was almost undetectable in neuronal cultures. Actin was used as a control for gel loading. (c) Confocal microscopy images of primary cultured astrocytes, neurons and N2a cells growing in medium with 30 mM glucose. Cells were processed for immunofluorescence analysis with glycogen antibodies (GLY). GFAP and TUJ1 antibodies were used as markers of glial and neuronal cells, respectively. All images were acquired using a 63 \times objective with an additional 1.4 confocal magnification.

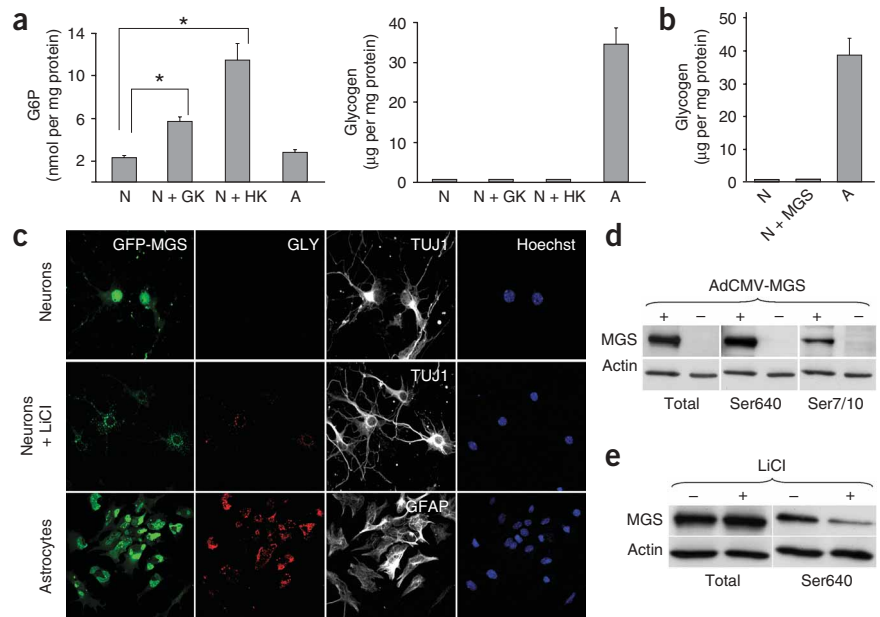
The inability of neurons to synthesize glycogen could be a consequence of a lack of sufficient intracellular concentrations of glucose-6-phosphate (G6P), the metabolite required for the activation of MGS^{21–23}, or of sufficient amounts of MGS in this cell type. However, a fivefold increase in the amount of intracellular G6P in primary cultured neurons by overexpression of glucokinase or hexokinase I did not result in glycogen synthase activation or glycogen accumulation (Fig. 2a). Similarly, overexpression of MGS in primary cultured neurons using recombinant adenoviruses did not increase glycogen deposition (Fig. 2b,c). These results indicate that the lack of glycogen accumulation in these cells was not a result of low levels of MGS or G6P. Similar results were obtained in N2a cells (Supplementary Fig. 1 online). MGS expressed in neurons localized mostly in the nucleus (Fig. 2c, upper), which is a characteristic of cells that are depleted of glycogen^{24,25}. In contrast, MGS in astrocytes clustered in the cytoplasm,

which is a typical location for this protein under conditions of active glycogen synthesis (Fig. 2c, lower).

Control of glycogen synthesis is achieved mainly through the inactivation of MGS by phosphorylation of multiple serine residues at the C and N termini by a range of kinases²⁶. Western blot analysis showed that MGS in primary cultured neurons and N2a cells was phosphorylated at the Ser640 and Ser7/10 residues, the phosphorylation sites that reduce the activity of the enzyme the most²⁶ (Fig. 2d and Supplementary Fig. 1). However, Ser640 can be effectively dephosphorylated by treating neurons with 20 mM LiCl (Fig. 2e), a glycogen synthase kinase 3 inhibitor²⁷. Concomitantly, dephosphorylated MGS altered its subcellular localization and accumulated at specific sites in the cytoplasm, coinciding with growing glycogen particles (Fig. 2c, middle panel and Supplementary Fig. 1). Incubation of primary cultured neurons with LiCl at therapeutic concentrations (1–2 mM) for up to 48 h did not produce any substantial effect on MGS.

Extensive MGS dephosphorylation at Ser640 and Ser7/10 was induced in primary cultured neurons and N2a cells by PTG (Fig. 3a and Supplementary Fig. 1), a regulatory subunit of protein

Figure 2 Effects of increased intracellular levels of G6P or overexpression of MGS. (a) Graphs show the intracellular levels of G6P (left) and the glycogen content (right) of neurons overexpressing glucokinase (N + GK) or hexokinase I (N + HK) (MOI 100) and uninfected neurons (N). A fivefold increase in the intracellular levels of G6P did not increase glycogen accumulation. G6P levels represent the mean \pm s.e.m. ($n = 5–7$) of three independent experiments. * $P < 0.001$ noninfected versus AdCMV-GK, AdCMV-HK I-infected. Glycogen content represents the mean \pm s.e.m. ($n = 6–10$) of three independent experiments. (b) Glycogen content (mean \pm s.e.m., $n = 6$) of three independent experiments in primary cultures of neurons and astrocytes. Glycogen was undetectable in noninfected and AdCMV-MGS-infected (N + MGS, MOI 100) neuronal cells. (c) Immunofluorescence analysis with GLY and specific markers of neurons (TUJ1) and astrocytes (GFAP). Cell nuclei were stained with Hoechst 33342. Cells were treated with AdCMV-GFP-MGS (MOI 50 for neurons and 5 for astrocytes). MGS-overexpressing neurons accumulated glycogen when treated with 20 mM LiCl for 24 h (middle). All images were acquired using a 63 \times objective with an additional 1.4 confocal magnification. (d) Western blot analysis of AdCMV-MGS-infected (+, MOI 100) versus noninfected (–) neurons. We used antibodies recognizing total MGS and phosphorylated MGS on Ser640 and Ser7/10. (e) Western blot analysis of MGS-overexpressing neurons incubated in the presence (+) or absence (–) of 20 mM LiCl (24 h) with antibodies to MGS and Ser640.



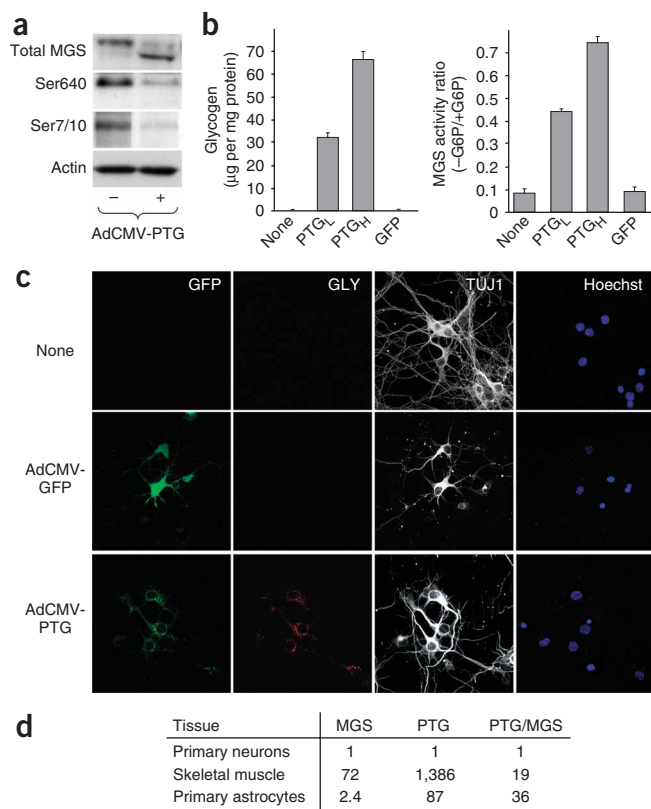


Figure 3 PTG expression activates neuronal MGS and results in glycogen accumulation. **(a)** Western blot analysis of neurons treated (+) or not (-) with AdCMV-PTG (MOI 100) and then incubated with antibodies that recognize total MGS and phosphorylated MGS on Ser640 and on Ser7/10. PTG overexpression stimulated the dephosphorylation of MGS at these sites. **(b)** Glycogen content and MGS activity ratio (-G6P/+G6P) of neurons treated with AdCMV-PTG at low (PTG_L, 50) and high (PTG_H, 100) MOI. None = noninfected neurons. PTG overexpression had a marked effect on the stimulation of neuronal glycogen deposition and MGS activity. Glycogen content represents the mean \pm s.e.m. ($n = 6-10$) of three independent experiments. MGS activity ratio represents the mean \pm s.e.m., $n = 6-12$, of three independent experiments. **(c)** Glycogen immunocytochemistry of primary cultures of neurons infected with AdCMV-PTG (MOI 50). TUJ1 and Hoechst 33342 staining were used as markers of neurons and nuclei, respectively. Glycogen accumulated in cell soma and in neurites. As a control for adenovirus infection, neurons were treated with AdCMV-GFP (MOI 50). All images were acquired using a 63 \times objective with an additional 1.4 confocal magnification. **(d)** RT-PCR. MGS and PTG transcript levels were compared with the values obtained in primary cultures of neurons, which were assigned a value of 1. The PTG/MGS transcript ratio in neurons was lower than the ratio in muscle or astrocytes.

essentially blocked by keeping MGS in a phosphorylated, inactive state. In this context, it is of interest that PTG is scarcely expressed in neurons³². The PTG-MGS transcript ratio was approximately 20-fold lower in neurons than in cells that normally accumulate glycogen (Fig. 3d).

Because Lafora bodies are composed of poorly branched glucose polymers, we complexed samples isolated from neuronal cells with iodine and recorded the spectra, as described³³, to measure the degree of ramification of the glycogen produced in the experiments described above. Shifting of the absorption maximum to a higher wavelength is indicative of less branching. Normal glycogen gave a peak at 483 nm, whereas that isolated from N2a or primary cultured neurons peaked at 511 nm, indicating that it was poorly branched.

Glycogen accumulation is pro-apoptotic in neuronal cells

To ascertain whether accumulation of this poorly branched glycogen causes alterations in neuronal cells, we examined whether apoptotic markers were present in primary cultured neurons that were forced to accumulate glycogen by overexpression of PTG. Glycogen-accumulating primary cultured neurons showed increased apoptosis compared with controls when measured by TUNEL staining (Fig. 4a) and active caspase-3 assays (Fig. 4b,c).

phosphatase 1 that promotes the activation of MGS²⁸⁻³⁰ and that interacts with laforin³¹. This dephosphorylation was accompanied by a marked increase in glycogen accumulation throughout the soma, neurites and axons (Fig. 3b,c and Supplementary Fig. 1). Like LiCl, PTG induced the intracellular relocation of MGS, which became clustered in the cytoplasm, colocalizing with glycogen particles (data not shown). The activation state of MGS increased in neurons overexpressing PTG, reaching values that were close to those of full activation (Fig. 3b and Supplementary Fig. 1), and the enzyme showed increased electrophoretic mobility, which is characteristic of the activated (dephosphorylated) enzyme (Fig. 3a and Supplementary Fig. 1). Taken together, these findings demonstrate that neurons have the appropriate machinery to synthesize glycogen, but this system is

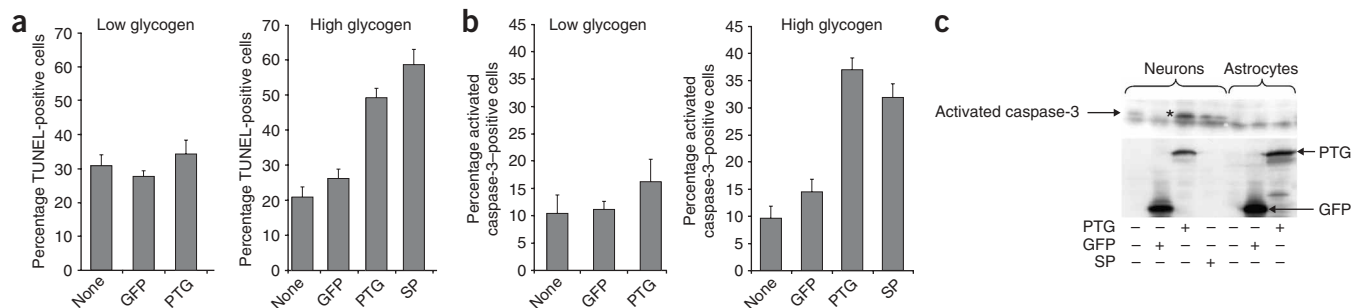


Figure 4 Accumulation of glycogen promotes apoptosis in primary cultured neurons. **(a)** Percentage of TUNEL-positive neurons accumulating low and high levels of glycogen. Glycogen accumulation was modulated by expression of PTG (AdCMV-PTG, MOI 50) for 24 h (low glycogen) or 96 h (high glycogen). GFP in the figure refers to AdCMV-GFP-treated cells (MOI 50). We used a 24-h treatment with 0.1 μ M staurosporine as a positive control (SP). The percentage of TUNEL-positive cells was estimated in 8-14 fields (mean \pm s.e.m.) in three coverslips for each treatment condition (500-600 total cells). **(b)** Percentage of activated caspase-3-positive neurons (mean \pm s.e.m., 8-14 coverslip fields of three independent experiments, 550-600 total cells) in the same experimental conditions shown in **a**. **(c)** Western blot analysis of activated caspase-3 in primary cultured neurons and astrocytes in the same experimental conditions shown in **a** (96 h). Asterisk indicates the activated caspase-3. The lower panel shows a western blot with the GFP antibody.

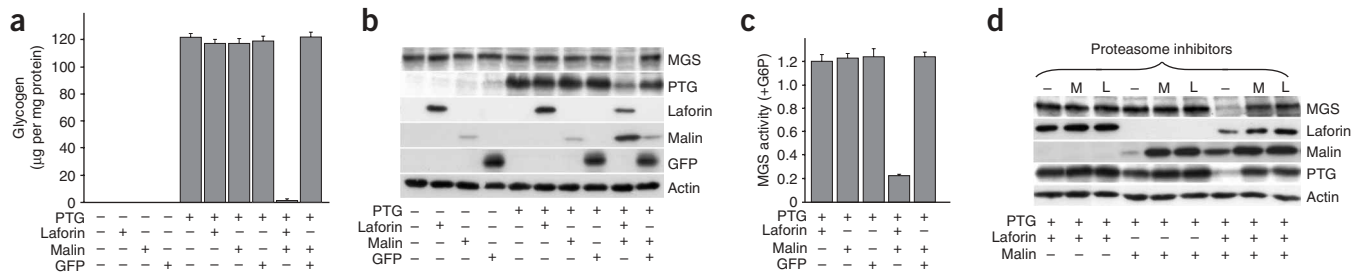


Figure 5 Blockade of glycogen synthesis by laforin and malin. **(a)** Glycogen content of N2a cells (mean \pm s.e.m., $n = 14$ – 23 , of 6 independent experiments) incubated with the recombinant adenoviruses indicated, used at a MOI of 20, with the exception of AdCMV-PTG, which was used at a MOI of 5. Malin and laforin coexpression blocked the glycogen accumulation induced by PTG. **(b)** Western blot analysis of N2a cells treated with recombinant adenoviruses in the same conditions as described in **a**. Note that MGS, PTG and laforin signals were markedly reduced when laforin and malin were coexpressed. Actin was used as a control for gel loading. **(c)** Total MGS activity (+G6P) of N2a cells (mean \pm s.e.m., $n = 6$ – 8 , of three independent experiments) after infection with AdCMV-PTG, AdCMV-laf, AdCMV-malin and AdCMV-GFP in the same conditions as described in **a**. Total MGS activity was reduced when laforin was coexpressed with malin. **(d)** Western blot analysis of N2a cells incubated with the recombinant adenoviruses indicated in the figure and treated with the proteasome inhibitors MG-132 1 μ M (M) or lactacystin 5 μ M (L) for 18 h. Proteasome inhibitors were added 4 h after the incubation with the adenoviruses. Cells were processed for western blot 22 h after infection. All of the viruses were used at a MOI of 10, except for AdCMV-PTG, which was used at a MOI of 2. Treatment with proteasome inhibitors blocked the degradation of MGS, laforin and PTG observed in cells expressing both malin and laforin and increased the total amount of malin.

In contrast, astrocytes expressing the same amount of PTG, and therefore synthesizing high levels of glycogen, did not show an activation of caspase-3 (Fig. 4c). Therefore, glycogen deposition triggered apoptosis specifically in cultured neurons.

The laforin-malin complex downregulates glycogen synthesis

To determine the role of laforin and malin in the generation of Lafora bodies, we analyzed whether these proteins have the capacity to modulate the PTG-induced accumulation of glycogen in neuronal cells. When laforin and malin were separately coexpressed with PTG in these cells, we did not observe an effect on PTG-induced glycogen accumulation (Fig. 5a and Supplementary Fig. 2 online). However, when both laforin and malin were coexpressed simultaneously with PTG, they completely blocked the activation of glycogen synthesis (Fig. 5a and Supplementary Fig. 2). In addition, we detected a marked reduction of MGS and PTG levels (Fig. 5b and Supplementary Fig. 2). The levels of laforin were also diminished, although to a lesser extent (Fig. 5b). In contrast, the amount of malin was substantially increased when it was coexpressed with laforin, suggesting that malin is stabilized by laforin. Therefore, malin levels were inversely correlated with those of MGS, PTG and laforin (Fig. 5b). The reduction of MGS protein levels was correlated with a sixfold decrease in MGS activity in cells expressing both laforin and malin compared with cells expressing laforin alone (Fig. 5c). The effects of malin and laforin on MGS and PTG were specific, as other proteins involved in glycogen metabolism, such as hexokinase I or glycogen synthase kinase 3, were not degraded by the combined action of laforin and malin (data not shown). The proteasome inhibitors MG-132 and lactacystin³⁴ blocked the decrease of MGS, PTG and laforin levels that was induced by the malin-laforin complex (Fig. 5d and Supplementary Fig. 2). Quantitative real-time PCR (RT-PCR) analysis confirmed that MGS, laforin and PTG transcript levels were unaffected, indicating that the changes in MGS and PTG protein levels were a consequence of protein degradation through the ubiquitin-proteasome pathway and were not caused by alterations at the transcription level (data not shown). These data suggest that the laforin-malin complex is important in the modulation of MGS and PTG levels. Proteasome-dependent degradation of laforin, together with PTG and MGS, may act as a safety switch; that is, when laforin levels are reduced, no laforin-malin complexes are formed, and

therefore MGS and PTG degradation will not occur. In addition, the amount of malin expressed in the absence of laforin was higher when these proteasome inhibitors were present. This observation suggests that malin is also degraded through the ubiquitin-proteasome pathway (Fig. 5d).

In a survey of individuals with Lafora disease, we identified a malin mutation (D146N) that specifically disrupts the interaction between laforin and malin without altering the E3 ubiquitin ligase activity of the latter (M.C. Solaz-Fuster, J.V. Gimeno-Alcañiz, S.R., M.E. Fernández-Sánchez, B.G.-F., O.C.-G., D.V., J.D., M.G.-R., M. Sánchez-Piriz, C. Aguado, E. Knecht, J. Serratos, J.J.G., P. Sanz and S.R.d.C., unpublished data). Notably, D146N did not impair PTG-induced glycogen accumulation in the presence of laforin (Fig. 6a) and, in contrast to wild-type malin, failed to induce the degradation of MGS and PTG (Fig. 6b). Therefore, the malin-laforin interaction is crucial for the action of these two proteins on neuronal glycogen metabolism.

If laforin and malin are required to decrease the levels of MGS and PTG, the absence of these proteins in individuals with Lafora disease should result in increased MGS and PTG levels. To test this, we mimicked the pathological condition by silencing laforin expression in neuronal cells using short interfering RNA (siRNA) oligonucleotides (Fig. 6c). The knockdown of laforin by two distinct siRNAs caused a marked increase in MGS and PTG levels compared with those in cells transfected with control siRNA (Fig. 6d,e). More glycogen accumulated in these cells under glycolytic conditions (Fig. 6f). These results establish the involvement of the laforin-malin system in the control of MGS and PTG stability and glycogen synthesis.

DISCUSSION

Our findings demonstrate the existence of a previously unknown regulatory mechanism for glycogen accumulation in neurons, which operates through the proteasome-mediated degradation of both MGS and PTG, with the latter being the key protein for MGS activation (see schematic in Supplementary Fig. 3 online). MGS is a highly regulated enzyme. It is activated by G6P and inactivated by phosphorylation at multiple sites³⁵. Furthermore, it is also regulated by changes in its subcellular localization in response to the metabolic status of the cell²⁴. The mechanism demonstrated here, mediated by the laforin-malin complex, represents an additional control step that is superimposed on

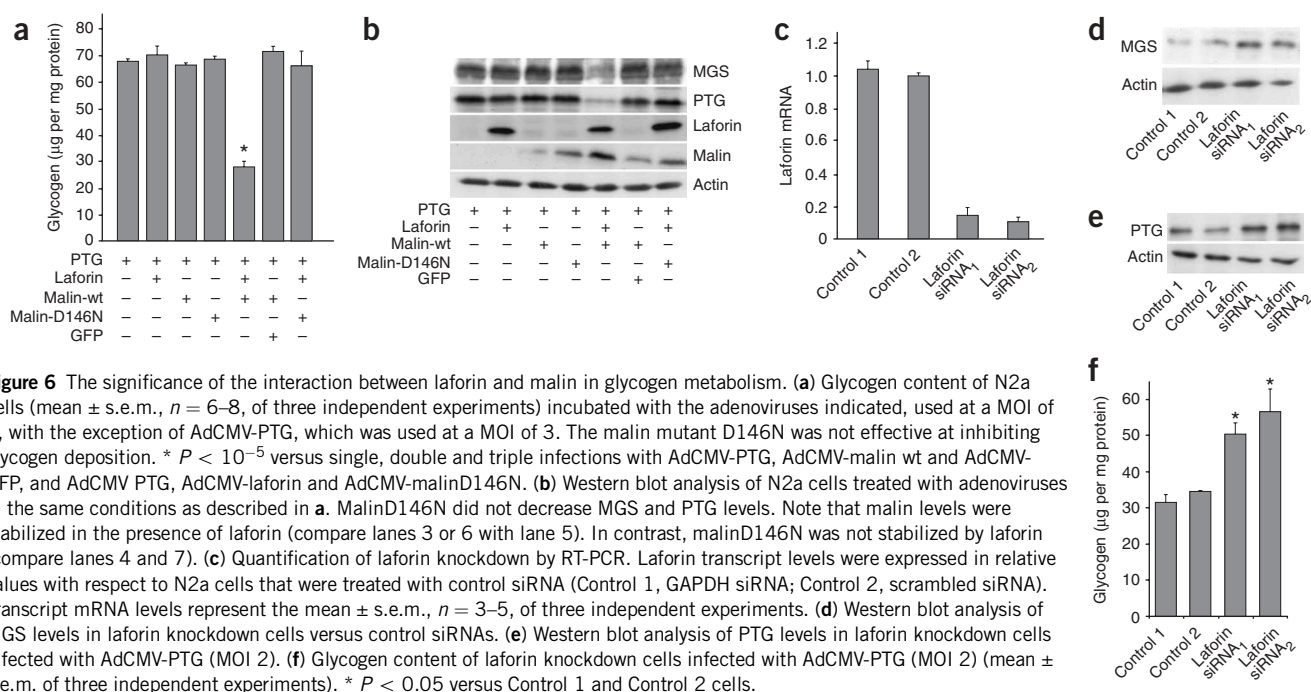


Figure 6 The significance of the interaction between laforin and malin in glycogen metabolism. **(a)** Glycogen content of N2a cells (mean \pm s.e.m., $n = 6-8$, of three independent experiments) incubated with the adenoviruses indicated, used at a MOI of 5, with the exception of AdCMV-PTG, which was used at a MOI of 3. The malin mutant D146N was not effective at inhibiting glycogen deposition. * $P < 10^{-5}$ versus single, double and triple infections with AdCMV-PTG, AdCMV-malin wt and AdCMV-GFP, and AdCMV PTG, AdCMV-laforin and AdCMV-malinD146N. **(b)** Western blot analysis of N2a cells treated with adenoviruses in the same conditions as described in **a**. MalinD146N did not decrease MGS and PTG levels. Note that malin levels were stabilized in the presence of laforin (compare lanes 3 or 6 with lane 5). In contrast, malinD146N was not stabilized by laforin (compare lanes 4 and 7). **(c)** Quantification of laforin knockdown by RT-PCR. Laforin transcript levels were expressed in relative values with respect to N2a cells that were treated with control siRNA (Control 1, GAPDH siRNA; Control 2, scrambled siRNA). Transcript mRNA levels represent the mean \pm s.e.m., $n = 3-5$, of three independent experiments. **(d)** Western blot analysis of MGS levels in laforin knockdown cells versus control siRNAs. **(e)** Western blot analysis of PTG levels in laforin knockdown cells infected with AdCMV-PTG (MOI 2). **(f)** Glycogen content of laforin knockdown cells infected with AdCMV-PTG (MOI 2) (mean \pm s.e.m. of three independent experiments). * $P < 0.05$ versus Control 1 and Control 2 cells.

the previously known ones described above, and adds a further level of complexity to the control of glycogen synthesis. Although prevalent in neurons, this mechanism is probably involved in the regulation of glycogen synthesis more generally, as laforin and malin are not restricted to neurons. This mechanism probably serves to prevent excessive glycogen accumulation in certain tissues or under specific physiological conditions.

Furthermore, we demonstrate here that, against general belief, neurons have the machinery to synthesize glycogen, but this capacity is silenced by the inactivation of neuronal MGS through extensive phosphorylation and by the mechanism described here, which further ensures the blockage of glycogen synthesis by degrading both MGS and PTG. Altogether, these apparently redundant control mechanisms for glycogen synthesis may reflect the need to prevent glycogen accumulation in neurons. Neurons do not express detectable amounts of glycogen phosphorylase, the key enzyme for glycogen degradation. Therefore, the degradation of glycogen, should it accumulate, would not be feasible. Furthermore, when MGS becomes active, neurons accumulate poorly branched glycogen (polyglucosan). This observation illustrates the necessity of strictly controlling MGS activity in neurons.

As we have shown, deposition of this poorly branched glycogen is associated with deleterious effects in neuronal cells, as it activates the apoptotic program. Consequently, the previously unknown regulatory mechanism for glycogen synthesis that we report here is probably critical for preventing the accumulation of a dangerous molecule in the cytoplasm of neurons. Disturbance of this mechanism, as a consequence of loss-of-function mutations in laforin or malin, would explain the accumulation of intracellular inclusion bodies of glycogen-like composition in neurons (and in other cell types). We do not know the extent to which this phenomenon may be responsible for the cardinal clinical manifestations of Lafora disease. Although our results are consistent with the hypothesis that glycogen deposition triggers the alterations of neuronal function in Lafora disease, we cannot exclude the possibility that other potential targets of the laforin-malin complex are also involved in the pathogenesis of this disease. Whether this complex also triggers the degradation of other proteins is unknown.

In addition, our results raise the question of why neurons have maintained MGS expression throughout evolution if it must be kept strictly inactive under normal conditions. One possibility is that the genomic structure of the MGS gene (*Gys1*) does not allow for the silencing of MGS expression in neurons without interfering with the expression of other relevant neuronal genes or with the expression of MGS in other cell types. Alternatively, MGS may have a second, as yet undiscovered, fundamental function in neurons.

METHODS

Primary cultures of neurons and astrocytes. We obtained telencephalic neuron cultures from mouse embryos at embryonic day 16 (OF1 mice, Charles River Laboratories) as described³⁶ (Supplementary Methods online). These experiments were approved by the Barcelona Science Park's Animal Experimentation Committee and were carried out in accordance with the European Community Council Directive and the US National Institutes of Health guidelines for the care and use of laboratory animals. Enzymes and biochemical reagents were from Sigma, unless otherwise indicated. All other chemicals were of analytical grade. We cultured cells in serum-free Neurobasal medium (Invitrogen) supplemented with 2 mM L-glutamine (Invitrogen), 30 mM D-glucose, 5 mM NaHCO₃ (Invitrogen), penicillin (100 U ml⁻¹, Invitrogen), streptomycin (100 mg ml⁻¹, Invitrogen) and B27 supplement diluted 1:50 (Invitrogen). After 1 d of culture, we treated cells with uridine (50 µg ml⁻¹) and 5-fluoro-2'-deoxyuridine (20 µg ml⁻¹) to minimize the contamination by astrocytes. Primary cultures of neurons were infected at 5 d in culture for 12 h with adenoviruses at diverse multiplicities of infection (MOI) depending on the experiments. After removal of the virus-containing media, infected cells were maintained for 48 h in neuronal culture medium. For primary cultures of astrocytes, we cultured dissociated cells in Neurobasal medium supplemented with 2 mM L-glutamine, 30 mM D-glucose, 5 mM NaHCO₃, penicillin (100 U ml⁻¹), streptomycin (100 mg ml⁻¹), 5% horse serum and 5% fetal bovine serum (FBS). Primary cultures of astrocytes were incubated for 2 h with adenoviruses at diverse MOIs. After removal of the virus-containing media, astrocytes were incubated for 48 h with astrocyte culture medium.

N2a cells. We cultured N2a cells (American Type Culture Collection, CCL-131) in Dulbecco's modified eagle medium (DMEM, Invitrogen) supplemented with

2 mM L-glutamine, 25 mM D-glucose, penicillin (100 U ml⁻¹), streptomycin (100 mg ml⁻¹) and 10% FBS. Cells differentiated after being cultured for 72 h in FBS-free DMEM (with supplements). N2a cells were incubated for 2 h with adenoviruses at various MOIs. After removal of the virus-containing media, N2a cells were incubated for 48 h with N2a differentiation medium.

Preparation of recombinant adenovirus. Recombinant adenoviruses coding for rat liver glucokinase (AdCMV-GK)³⁷, rat liver hexokinase I (AdCMV-HKI)³⁷, green fluorescent protein (GFP) (AdCMV-GFP)²², human MGS (AdCMV-MGS)²² and human MGS fused to GFP (AdCMV-GFP-MGS)²⁵ have been described. We generated recombinant adenoviruses coding for the mouse PTG fused to GFP (AdCMV-PTG), human laforin (AdCMV-laf), wild-type (wt) human malin (AdCMV-malin) and mutant D146N human malin (AdCMV-malinD146N) fused to hemagglutinin epitope (HA). We obtained the coding sequence for PTG by amplification of mouse hepatocyte genomic DNA using the oligonucleotide primers 5'-CCG AAT TCG GNA CGA GAT GTG CTA GAT CC-3' and 5'-CGC CAG TGT GCT GGA ATT CTC AAG TAG-3'. The coding sequence for PTG was then ligated into the pEGFP-C1 vector (Clontech), which was previously digested with *Bgl*III. The generation of the pCINeo-Laforin vector was described previously³¹. The coding sequence of human malin was amplified from human spleen genomic DNA by PCR using the oligonucleotide primers 5'-GGA TCC TAT GGC GGC CGA AGC-3' and 5'-GAG ATC TCA CAA TTC ATT AAT GGC AGA C-3', and was cloned into the mammalian expression vector pcDNA3, which contained an N-terminal HA tag. This pcDNA3-Malin wt-HA vector was used as the template for the introduction of mutation D146N by PCR, using the QuikChange Site-Directed Mutagenesis Kit (Stratagene). Then pEGFP-PTG, pCINeo-Laforin, pcDNA3-Malin wt-HA and pcDNA3-Malin D146N-HA vectors were used as templates for subcloning all of the selected cDNAs into the pAC.CMVpLpA plasmid³⁸ using the BD In Fusion PCR Cloning kit (Clontech) and appropriate oligonucleotides (5'-CGA GCT CCG TAC CCG GGA TAC CAC CAT GGC C-3' and 5'-CTG CAG GTC CAG TCT AGA TCA GCG AGC TCT AG-3' for laforin, 5'-CGA GCT CGG TAC CCG GGC GAC TCA CTA TAG GC-3' and 5'-CTG CAG GTC GAC TCT AGT CGA CTC TAG ACC AG-3' for wt malin-HA and malin D146N-HA, and 5'-CGA GCT CGG TAC CCG GGC GGC TAC CGG TCG CC-3' and 5'-AAG CTA TAG CTA CTT GCT AGA GTC GAC CTG CAG-3' for PTG-GFP).

To obtain the infective particles, human kidney 293 cells (cultured in DMEM supplemented with 10% FBS) were cotransfected with pAC.CMV plasmids containing the PTG-GFP, laforin, wt malin-HA or malin D146N-HA cDNAs and the pJM17 plasmid³⁹, and then amplified³⁸. We confirmed the absence of errors by extracting and sequencing viral DNA³⁸ from all of the adenoviruses generated.

RNA interference. We used two independent siRNAs to target laforin: laforin siRNA₁ (Ambion, predesigned siRNA#16708: sense, 5'-GCA CAA CAA GAC UUU UCU Ctt-3', and antisense, 5'-GAG AAA AGU CUU GUU GUG Ctt-3') and laforin siRNA₂ (Custom SMARTpool siRNA designed to target laforin, Dharmacon). We used GAPDH human, mouse and rat siRNAs as positive controls and Negative Control #1 siRNA (Ambion, catalog #4624) as a negative control. We transfected a concentration of 100 nM of each siRNA into N2a cells using Lipofectamine 2000 (Invitrogen), following the manufacturer's instructions. We measured the efficiency of laforin knockdown by RT-PCR analysis.

Electrophoresis and immunoblotting. Cell-culture plates were processed for protein extract preparation (Supplementary Methods). Proteins were resolved by 10% SDS-PAGE, transferred onto a nitrocellulose membrane (Schleicher and Schuell) and probed with the following antibodies: rabbit antibody to human MGS (MGS3), which recognizes MGS independently of its phosphorylation state²⁵, sheep antibody to MGS phosphorylated on Ser7 and 10 (PGSser7/10, a gift from D.G. Hardie, University of Dundee, UK)⁴⁰, rabbit antibody to MGS phosphorylated on Ser640 (PGSser641, Cell Signaling), rabbit antibody to glial fibrillary acidic protein (GFAP, DakoCytomation), rabbit antibody to GFP (Immunokontakt), mouse antibody to β -actin, mouse antibody to HA and mouse antibody to laforin. Antibody to brain glycogen phosphorylase was produced by Eurogentec:

chickens were immunized against a peptide at the C terminus (GVEPSDLQIPPPNLPKD, amino acids 826–842) of mouse brain glycogen phosphorylase. For further details about the secondary antibodies used in this study see the **Supplementary Methods**.

Immunocytochemistry. Cells seeded on poly-L-lysine-coated coverslips were fixed for 30 min in PBS containing 4% (w/v) paraformaldehyde. After fixation, cells were incubated with NaBH₄ (1 mg ml⁻¹) for 10 min and permeabilized for 20 min with PBS containing 0.2% (v/v) Triton X-100. Blocking and incubation with the primary and secondary antibodies were carried out as previously described²⁵. Coverslips were washed, air-dried and mounted onto glass slides using Mowiol as mounting medium. We used primary antibodies to MGS3 and GFAP, mouse antibody to β -III-tubulin (TUJ1) and a monoclonal antibody against glycogen (a gift from O. Baba, Tokyo Medical and Dental University)⁴¹. In some cases, nuclei were stained with Hoechst 33342 (Molecular Probes). For information about the secondary antibodies used, see the **Supplementary Methods**. Fluorescence images were obtained with a Leica SPlI Spectral microscope (Leica Lasertechnik). The light source was an argon/krypton laser (75 mW), and optical sections (0.1 μ m) were obtained.

Apoptosis assays. Neurons seeded onto poly-L-lysine-coated coverslips were fixed for 30 min in PBS containing 4% (w/v) paraformaldehyde and processed for TUNEL or active caspase-3 staining. TUNEL assays were carried out using the ApopTag Peroxidase *in situ* Apoptosis Detection Kit (Chemicon), following the manufacturer's instructions. Active caspase-3-positive cells were visualized by immunocytochemistry using the cleaved caspase-3 antibody (Cell Signaling) (Supplementary Methods). The TUNEL- and active caspase-3-positive cells were photographed with a Nikon Eclipse E-600 microscope using a 40 \times objective. The percentage of positive cells was estimated in 8–14 fields from each of three coverslips (three independent experiments) for each treatment condition (500–600 total cells). Total number of cells was evidenced after staining of nuclei with Hoechst 33342.

RNA purification and retro-transcription. Total RNA was isolated from mouse tissue and reverse transcribed as described in the **Supplementary Methods**. A series of specific primers were designed to specifically amplify a fragment of the coding sequence of mouse MGS, LGS and GFAP (Supplementary Methods).

Quantitative RT-PCR. We followed the standard RT-PCR protocol of the ABI Prism 7700 Detection System, together with the ready-made TaqMan primer and probe sets (Applied Biosystems). Each sample was analyzed in triplicate wells with 30 ng of first-strand cDNA in a total reaction volume of 20 μ l. The temperature profile consisted of 40 cycles of 15 s at 95 $^{\circ}$ C and 1 min at 60 $^{\circ}$ C. Data was analyzed with the comparative 2 $\Delta\Delta$ Ct method using ribosomal 18S as endogenous control.

Metabolite determinations. To measure glycogen content, we scraped cell monolayers into 30% KOH and heated the extract for 15 min at 100 $^{\circ}$ C. We measured glycogen as described previously⁴². To assess glycogen branching, we used a previously described method based on the iodine absorption spectrum³³. The intracellular concentration of G6P was measured by a spectrophotometric assay⁴³.

Determination of MGS activity. Cell-culture plates were processed as described in the **Supplementary Methods**. Protein concentration was measured by the Bradford method⁴⁴. MGS activity was measured in homogenates in the absence or presence of 6.6 mM G6P, as described previously⁴⁵. The activity measured in the absence of G6P represents the active form of MGS (I or a form), whereas the activity measured in the presence of 6.6 mM G6P represents total MGS activity. The -G6P/+G6P activity ratio is a nonlinear measurement of the activation state of the enzyme. Values below 0.1 indicate an essentially fully inactive enzyme, whereas those above 0.7 are equivalent to full activation⁴⁶.

Statistical analysis. Results were analyzed for significance by ANOVA and unpaired Student's *t* test. *P* < 0.05 was considered to be significant.

Note: Supplementary information is available on the Nature Neuroscience website.

ACKNOWLEDGMENTS

We thank J. Massagué for providing a critical review of the manuscript, P. Sanz and J.M. Serratosa for their advice, A. Adrover and E. Veza for their technical support, and T. Yates for correcting the manuscript. We also thank R.R. Gomis for the AdCMV-PTG virus, O. Baba for the monoclonal antibody to glycogen and D.G. Hardy for the gift of the PG5ser7/10 antibody. This study was supported by grants from the *Fundació La Caixa*, *Fundació La Marató de TV3*, *Fundación Marcelino Botín*, the Spanish Ministry of Education and Science (SAF2005-00913; BFU2005-02253) and the *Instituto de Salud Carlos III* (CIBER-ER; RD06/0015/0030).

AUTHOR CONTRIBUTIONS

D.V. conducted most of the experiments, data analysis and interpretation. S.R. generated the AdCMV-laf, AdCMV-malin and AdCMV-malinD146N recombinant adenoviruses. D.C. carried out the RT-PCR experiments. L.P. contributed to the primary neuron cultures and the apoptosis assays. J.V. carried out the analysis of glycogen branching. S.R., D.C. and J.V. also contributed to other experiments. B.G.-F., O.C.-G., E.F.-S. and I.M.-F. generated the monoclonal laforin antibody, pCIneo-Laforin vector and pcDNA3-Malin-HA vector. J.D. supervised several experiments and the data analysis, and contributed to writing the manuscript. M.G.-R. supervised the western blot and immunofluorescence experiments. E.S. contributed with his knowledge of the nervous system. S.R.d.C. and J.J.G. planned and supervised the project, co-wrote the manuscript and contributed to every aspect of the project.

Published online at <http://www.nature.com/natureneuroscience>

Reprints and permissions information is available online at <http://npg.nature.com/reprintsandpermissions>

- Brown, A.M. Brain glycogen re-awakened. *J. Neurochem.* **89**, 537–552 (2004).
- Cavanagh, J.B. Corpora-amyloidea and the family of polyglucosan diseases. *Brain Res. Brain Res. Rev.* **29**, 265–295 (1999).
- Berkovic, S.F., Andermann, F., Carpenter, S. & Wolfe, L.S. Progressive myoclonus epilepsies: specific causes and diagnosis. *N. Engl. J. Med.* **315**, 296–305 (1986).
- Lafora, G.R. Über das korkornen amyloider körpchen im innern der ganglienzellen; zugleich ein zum studium der amyloiden substanz im nervensystem. *Virchows Arch. Pathol. Anat.* **205**, 294–303 (1911).
- Lafora, G.R. & Glueck, B. Beitrag zur histopathologie der myklonischen epilepsie. *Z. Gesamte Neurol. Psychiatr.* **6**, 1–14 (1911).
- Collins, G.H., Cowden, R.R. & Nevis, A.H. Myoclonus epilepsies with Lafora bodies. An ultrastructural and cytochemical study. *Arch. Pathol.* **86**, 239–254 (1968).
- Sakai, M., Austin, J., Witmer, F. & Trueb, L. Studies in myoclonus epilepsies (Lafora body form). II. Polyglucosans in the systemic deposits of myoclonus epilepsies and in corpora amyloidea. *Neurology* **20**, 160–176 (1970).
- Acharya, J.N., Satishchandra, P. & Shankar, S.K. Familial progressive myoclonus epilepsies: clinical and electrophysiologic observations. *Epilepsia* **36**, 429–434 (1995).
- Berkovic, S.F., Cochiuș, J., Andermann, E. & Andermann, F. Progressive myoclonus epilepsies: clinical and genetic aspects. *Epilepsia* **34** (Suppl 3): S19–S30 (1993).
- Kobayashi, K., Iyoda, K., Ohtsuka, Y., Ohtahara, S. & Yamada, M. Longitudinal clinicoelectrophysiologic study of a case of Lafora disease proven by skin biopsy. *Epilepsia* **31**, 194–201 (1990).
- Minassian, B.A. Lafora's disease: towards a clinical, pathologic and molecular synthesis. *Pediatr. Neurol.* **25**, 21–29 (2001).
- Shahwan, A., Farrell, M. & Delanty, N. Progressive myoclonic epilepsies: a review of genetic and therapeutic aspects. *Lancet Neurol.* **4**, 239–248 (2005).
- Van Heycop Ten Ham, M.W. Lafora disease, a form of progressive myoclonus epilepsies. *Handb. Clin. Neurol.* **15**, 382–422 (1974).
- Minassian, B.A. *et al.* Mutations in a gene encoding a novel protein tyrosine phosphatase cause progressive myoclonus epilepsies. *Nat. Genet.* **20**, 171–174 (1998).
- Minassian, B.A. *et al.* Mutation spectrum and predicted function of laforin in Lafora's progressive myoclonus epilepsies. *Neurology* **55**, 341–346 (2000).
- Serratosa, J.M. *et al.* A novel protein tyrosine phosphatase gene is mutated in progressive myoclonus epilepsies of the Lafora type (EPM2). *Hum. Mol. Genet.* **8**, 345–352 (1999).
- Wang, J., Stuckey, J.A., Wishart, M.J. & Dixon, J.E. A unique carbohydrate binding domain targets the lafora disease phosphatase to glycogen. *J. Biol. Chem.* **277**, 2377–2380 (2002).
- Ganesh, S., Puri, R., Singh, S., Mittal, S. & Dubey, D. Recent advances in the molecular basis of Lafora's progressive myoclonus epilepsies. *J. Hum. Genet.* **51**, 1–8 (2006).
- Chan, E.M. *et al.* Mutations in NHLRC1 cause progressive myoclonus epilepsies. *Nat. Genet.* **35**, 125–127 (2003).
- Gentry, M.S., Worby, C.A. & Dixon, J.E. Insights into Lafora disease: malin is an E3 ubiquitin ligase that ubiquitinates and promotes the degradation of laforin. *Proc. Natl. Acad. Sci. USA* **102**, 8501–8506 (2005).
- Ferrer, J.C. *et al.* Control of glycogen deposition. *FEBS Lett.* **546**, 127–132 (2003).
- Gomis, R.R., Cid, E., Garcia-Rocha, M., Ferrer, J.C. & Guinovart, J.J. Liver glycogen synthase but not the muscle isoform differentiates between glucose 6-phosphate produced by glucokinase or hexokinase. *J. Biol. Chem.* **277**, 23246–23252 (2002).
- Skurat, A.V., Dietrich, A.D. & Roach, P.J. Glycogen synthase sensitivity to insulin and glucose-6-phosphate is mediated by both NH₂- and COOH-terminal phosphorylation sites. *Diabetes* **49**, 1096–1100 (2000).
- Ferrer, J.C., Baque, S. & Guinovart, J.J. Muscle glycogen synthase translocates from the cell nucleus to the cytosol in response to glucose. *FEBS Lett.* **415**, 249–252 (1997).
- Cid, E., Cifuentes, D., Baque, S., Ferrer, J.C. & Guinovart, J.J. Determinants of the nucleocytoplasmic shuttling of muscle glycogen synthase. *FEBS J.* **272**, 3197–3213 (2005).
- Skurat, A.V., Wang, Y. & Roach, P.J. Rabbit skeletal muscle glycogen synthase expressed in COS cells. Identification of regulatory phosphorylation sites. *J. Biol. Chem.* **269**, 25534–25542 (1994).
- MacAulay, K. *et al.* Use of lithium and SB-415286 to explore the role of glycogen synthase kinase-3 in the regulation of glucose transport and glycogen synthase. *Eur. J. Biochem.* **270**, 3829–3838 (2003).
- Printen, J.A., Brady, M.J. & Saltiel, A.R. PTG, a protein phosphatase 1-binding protein with a role in glycogen metabolism. *Science* **275**, 1475–1478 (1997).
- Fong, N.M. *et al.* Identification of binding sites on protein targeting to glycogen for enzymes of glycogen metabolism. *J. Biol. Chem.* **275**, 35034–35039 (2000).
- Berman, H.K., O'Doherty, R.M., Anderson, P. & Newgard, C.B. Overexpression of protein targeting to glycogen (PTG) in rat hepatocytes causes profound activation of glycogen synthesis independent of normal hormone- and substrate-mediated regulatory mechanisms. *J. Biol. Chem.* **273**, 26421–26425 (1998).
- Fernandez-Sanchez, M.E. *et al.* Laforin, the dual-phosphatase responsible for Lafora disease, interacts with R5 (PTG), a regulatory subunit of protein phosphatase 1 that enhances glycogen accumulation. *Hum. Mol. Genet.* **12**, 3161–3171 (2003).
- Allaman, I., Pellerin, L. & Magistretti, P.J. Protein targeting to glycogen mRNA expression is stimulated by noradrenaline in mouse cortical astrocytes. *Glia* **30**, 382–391 (2000).
- Schlamowitz, M. On the nature of rabbit liver glycogen. II. Iodine absorption spectrum. *J. Biol. Chem.* **190**, 519–527 (1951).
- Lee, D.H. & Goldberg, A.L. Proteasome inhibitors: valuable new tools for cell biologists. *Trends Cell Biol.* **8**, 397–403 (1998).
- Villar-Palasi, C. & Guinovart, J.J. The role of glucose-6-phosphate in the control of glycogen synthase. *FASEB J.* **11**, 544–558 (1997).
- Simo, S. *et al.* Reelin induces the detachment of postnatal subventricular zone cells and the expression of the Egr-1 through Erk1/2 activation. *Cereb. Cortex* **17**, 294–303 (2007).
- Seoane, J. *et al.* Glucose-6-phosphate produced by glucokinase, but not hexokinase I, promotes the activation of hepatic glycogen synthase. *J. Biol. Chem.* **271**, 23756–23760 (1996).
- Becker, T.C. *et al.* Use of recombinant adenovirus for metabolic engineering of mammalian cells. *Methods Cell Biol.* **43** (Pt A): 161–189 (1994).
- McGrory, W.J., Bautista, D.S. & Graham, F.L. A simple technique for the rescue of early region I mutations into infectious human adenovirus type 5. *Virology* **163**, 614–617 (1988).
- Hojlund, K. *et al.* Increased phosphorylation of skeletal muscle glycogen synthase at NH₂-terminal sites during physiological hyperinsulinemia in type 2 diabetes. *Diabetes* **52**, 1393–1402 (2003).
- Baba, O. [Production of monoclonal antibody that recognizes glycogen and its application for immunohistochemistry]. *Kokubyo Gakkai Zasshi.* **60**, 264–287 (1993).
- Chan, T.M. & Exton, J.H. A rapid method for the determination of glycogen content and radioactivity in small quantities of tissue or isolated hepatocytes. *Anal. Biochem.* **71**, 96–105 (1976).
- Lang, G. & Michal, G. D-glucose-6-phosphate and D-fructose-6-phosphate. in *Methods of Enzymatic Analysis* (ed. Bergmeyer, H. U.) 1238–1242 (Academic Press, New York, 1974).
- Bradford, M.M. A rapid and sensitive method for the quantitation of microgram quantities of protein utilizing the principle of protein-dye binding. *Anal. Biochem.* **72**, 248–254 (1976).
- Thomas, J.A., Schlender, K.K. & Lerner, J. A rapid filter paper assay for UDPglucose-glycogen glucosyltransferase, including an improved biosynthesis of UDP-14C-glucose. *Anal. Biochem.* **25**, 486–499 (1968).
- Guinovart, J.J. *et al.* Glycogen synthase: a new activity ratio assay expressing a high sensitivity to the phosphorylation state. *FEBS Lett.* **106**, 284–288 (1979).